Boundary-Layer Meteorology (2005) 116: 395–421
DOI 10.1007/s10546-005-0905-5

DEVELOPMENT OF A MULTI-LAYER URBAN CANOPY MODEL FOR THE ANALYSIS OF ENERGY CONSUMPTION IN A BIG CITY: STRUCTURE OF THE URBAN CANOPY MODEL AND ITS BASIC PERFORMANCE

HIROAKI KONDO[1,5,*], YUTAKA GENCHI[1], YUKIHIRO KIKEGAWA[2], YUKITAKA OHASHI[3], HIROSHI YOSHIKADO[1] and HIROSHI KOMIYAMA[4]
[1]*National Institute of Advanced Industrial Science and Technology, Tsukaba, Japan;* [2]*Meisei University, Hino, Japan;* [3]*Okayama University of Science, Okayama, Japan;* [4]*University of Tokyo, Tokyo, Japan;* [5]*National Institute of Advanced Industrial Science and Technology, Research Institute for Environmental Management Technology, AIST-west, 16-1, Onogawa, Tsukuba, Ibaraki, 305-8569, Japan*

(Received in final form 17 February 2005)

Abstract. A multilayer one-dimensional canopy model was developed to analyze the relationship between urban warming and the increase in energy consumption in a big city. The canopy model, which consists of one-dimensional diffusion equations with a drag force, has three major parameters: building width, distance between buildings, and vertical floor density distribution, which is the distribution of a ratio of the number of the buildings that are taller than some level to all the buildings in the area under consideration. In addition, a simplified radiative process in the canopy is introduced. Both the drag force of the buildings and the radiative process depend on the floor density distribution. The thermal characteristics of an urban canopy including the effects of anthropogenic heat are very complicated. Therefore, the focus of this research is mainly on the basic performance of an urban canopy without anthropogenic heat. First, the basic thermal characteristics of the urban canopy alone were investigated. The canopy model was then connected with a three-dimensional mesoscale meteorological model, and on-line calculations were performed for 10 and 11 August, 2002 in Tokyo, Japan. The temperature near the ground surface at the bottom of the canopy was considerably improved by the calculation with the canopy model. However, a small difference remained between the calculation and the observation for minimum temperature. Deceleration of the wind was well reproduced for the velocity at the top of the building by the calculation with the canopy model, in which the floor density distribution was considered.

Keywords: Drag force, Multi-layer urban canopy model, Radiation in the urban canopy, Urban heat island.

1. Introduction

The temperature increase due to anthropogenic heat discharge is a serious problem for energy use in a large urban area because the energy demand by

* E-mail: kondo-hrk@aist.go.jp

air-conditioning systems is accelerated and results in an increase of CO_2 emission through the consumption of fossil fuels. Akbari et al. (1990) showed a positive correlation between temperature and energy use in Los Angeles, California, U.S.A. A similar relationship was observed in the central part of Tokyo, Japan (Kikegawa et al., 2003). The correlation between temperature increase and energy use is apparent in summer; however, it is difficult to determine the cause of urban warming in a big city. Oke (1978) pointed out seven possibilities for warming in urban areas. One of the objectives of the present paper is to develop a method to quantitatively analyze the contribution of these factors in Tokyo, Japan, in order to develop a strategy to mitigate the excessive use of energy in summer. Tokyo has a population in excess of 8 million, and its diameter is about 40 km. There are many sub-central areas with heavy concentrations of office and commercial buildings.

Heat in urban areas arises primarily from solar insolation and anthropogenic sources. The amount of solar energy stored in a unit area depends on the structure, materials, and distribution of buildings, and the anthropogenic energy discharge depends on the distribution of human activity. Recently, urban heat island analyses using meteorological mesoscale models have been conducted with a 1–2 km grid interval (Ichinose et al., 1999; Urano et al., 1999). These mesoscale models treat a grid area as homogeneous, and their ground surface is usually of the slab-type (Kusaka et al., 2001). Since heat moving through vertical walls and insolation through windows of buildings are major heat sources for a building air-conditioning system, aside from internal heat sources in the building, the model developed here should be able to treat a three-dimensional structure of an urban area to some extent (Ashie et al., 1999). A three-dimensional wind-engineering model with a radiative process can be used to determine the thermal environment for each building (Murakami et al., 2000), which is another approach to the analysis; however, such systems are too time consuming for the analysis of an entire urban area. Heat storage is a major energy source in an urban area at night and more than one diurnal cycle will need to be calculated. Canopy parameterization (Masson, 2000; Martilli, 2002; Martilli et al., 2002;) appears to be a powerful tool for filling the gap between the grid scale of a mesoscale model and the building scale.

In the present paper, we develop a multi-layer one-dimensional urban canopy model that can be applied to a three-dimensional experiment. Kondo and Kikegawa (2003) have developed a combined model of the present canopy model and a building energy consumption model that calculates anthropogenic heat discharge dynamically in order to analyze the relationship between the temperature outside of a building and the amount of anthropogenic heat discharge. However, the performance of the canopy model itself has not be well investigated. In the present study, the basic characteristics of the climate in an urban canopy were examined with a one-

dimensional canopy model alone. The canopy model was then combined with a mesoscale meteorological model and applied to observational results in Tokyo. Although anthropogenic heat is a major source in an urban heat island, as mentioned above, an urban canopy and its effects on the urban thermal characteristics are quite complicated. Therefore, it is necessary to check the model performance step by step. In this comparison, anthropogenic heat is not considered, and a comparison with observations was made for the summer holiday period. A further comparison of the combined mesoscale and canopy models with a building energy-consumption model is under way.

2. The Canopy Model

2.1. Atmospheric layer

The canopy model consists of one-dimensional diffusion equations for momentum, potential temperature, and specific humidity. In the momentum equations, a similar idea for the diffusion and drag terms to those of Kondo and Akashi (1976), Sorbjan and Uliasz (1982), and Uno et al. (1989) is used for buildings.

$$\frac{\partial u}{\partial t} = \frac{1}{m}\frac{\partial}{\partial z}\left(K_m \cdot m \cdot \frac{\partial u}{\partial z}\right) - cau\left(\sqrt{u^2 + v^2}\right) + f(v - v_g), \tag{1}$$

$$\frac{\partial v}{\partial t} = \frac{1}{m}\frac{\partial}{\partial z}\left(K_m \cdot m \cdot \frac{\partial v}{\partial z}\right) - cav\left(\sqrt{u^2 + v^2}\right) - f(u - u_g). \tag{2}$$

Here, u and v are the wind velocity components in the east-west and north-south directions, respectively, and m is a volume porosity; K_m, c and a are discussed below.

We consider an urban block of up to 1 km square, in which buildings with an identical square bottom are assumed to be equally spaced in a north-south and east-west direction (Figure 1). The length of the square is b, and the distance between the buildings is d. We further assume that the four sidewalls of the buildings are exactly directed to the north, south, east, and west. The height of the buildings is not uniform, but the distribution of the height can be considered. We define the rate of actual buildings that occupy level z to all the buildings (floor density distribution, $0 \le P_b(z) \le 1$). $P_b(z) = 0$ means that there is no building at level z, and $P_b(z) = 1$ means that the entire building area (shaded in Figure 1) at z is actually occupied by buildings. The grid including buildings is considered as a porous medium. Since the equation is one-dimensional, volume porosity is equal to surface permeability. We then define volume porosity as,

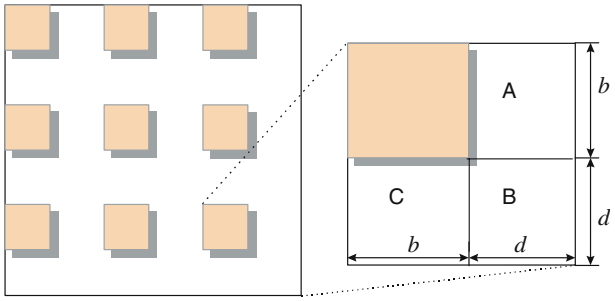

Figure 1. Location of the buildings in a canopy.

$$m = 1 - \left(\frac{b^2}{(d+b)^2}\right) P_b(z). \tag{3}$$

Here, c is a parameter depending on $\frac{b^2}{(d+b)^2}$ and derived from wind-tunnel experiments (Maruyama, 1991; Hagishima et al., 2001); a is a similar parameter to A_t in Uno et al. (1989), but, here, we consider the building floor density distribution $P_b(z)$, with

$$a = \frac{bP_b(z)}{(b+d)^2 - b^2 P_b(z)}, \tag{4}$$

where f is the Coriolis parameter, and u_g, v_g, the geostrophic wind components.

The equations for potential temperature and specific humidity are,

$$\frac{\partial \theta}{\partial t} = \frac{1}{m}\frac{\partial}{\partial z}\left(K_h m \frac{\partial \theta}{\partial z}\right) + \frac{1}{c_p \rho} Q_{AS}(z,t), \tag{5}$$

$$\frac{\partial q_v}{\partial t} = \frac{1}{m}\frac{\partial}{\partial z}\left(K_q m \frac{\partial q_v}{\partial z}\right) + \frac{1}{l\rho} Q_{AL}(z,t), \tag{6}$$

where θ, q_v, Q_{AS}, and Q_{AL} are the potential temperature, specific humidity, anthropogenic sensible heat, and anthropogenic latent heat, respectively. Both the sensible and latent anthropogenic heat depend on the time and height, and are dynamically calculated with building energy consumption models in Kondo and Kikegawa (2003). Here, c_p is the specific heat of air, ρ, the air density, and l, the latent heat of vaporization.

In the atmosphere, except for the surface layer (the lowest layer in the atmosphere), discussed in Section 2.3, turbulent diffusion coefficients are used. Gambo's formula (Gambo, 1978) is used for $R_f \leq R_{fc}$, where R_f is the flux Richardson number and $R_{fc} = 0.29$ is the critical Richardson number, so that

$$K_m = L^2 \left| \frac{\partial U}{\partial z} \right| \frac{S_M^{3/2}}{\sqrt{C}} (1 - R_f)^{\frac{1}{2}}, \tag{7}$$

$$K_h = K_q = L^2 \left| \frac{\partial U}{\partial z} \right| \frac{S_M^{1/2}}{\sqrt{C}} S_H (1 - R_f)^{\frac{1}{2}} \tag{8}$$

for $R_f < R_{fc}$. The scale length L is given by Watanabe and Kondo (1990) and was derived from the consideration of the forest canopy,

$$L(z) = 2\kappa^3 \frac{1}{ca} \{1 - \exp(-\eta)\}, \tag{9a}$$

$$\eta = ca \frac{z}{2\kappa^2}, \tag{9b}$$

where κ is the Karman constant. L above the canopy layer is limited by Blackadar's formula (Blackadar, 1968),

$$L \leq \frac{\kappa z}{1 + \frac{\kappa z}{L_0}}, \tag{10}$$

for $L_0 = 100\,\mathrm{m}$. When $R_f > R_{fc}$,

$$K_m = K_h = K_q = L^2 \left| \frac{\partial U}{\partial z} \right|, \tag{11}$$

where L is calculated using Equation (9).

2.2. Radiation

Although the model is one-dimensional, the heat budget at the surface is considered on the ground, roof, and each level of a building's wall in four separate directions. The following equation is solved on each surface.

$$c_w \rho_w \frac{dT_w}{dt} \delta = R_N + Q + lE + G, \tag{12}$$

where c_w and ρ_w are the heat capacity and density of the building's wall, roof, or ground, respectively, T_w, the temperature of the wall, roof, or ground surface, δ, the thickness of the first layer, and R_N, Q, lE, and G, respectively, the net radiative flux, sensible heat flux, and latent heat flux, which are released from walls, roofs, or ground surfaces, and the heat storage in a building's walls, which may partly intrude into the rooms of the buildings or into the ground.

The calculation of the net radiation on each surface is one of the most complicated and time-consuming elements of such a model. For the shortwave flux, R_{NS}, we consider direct solar insolation, diffuse solar insolation from the sky, and reflection from the surface. Multiple reflection may be an important process in the urban block canyon; however, the reflection in the canyon is considered only once due to the complexity of the three-dimensional geometry.

$$R_{NS} = (1 - ref)\{rI_d + s_{vf}\,(S_p - I_p)\} + \sum_j s_{wbj} ref_j \{r_j I_d + s_{vfj}(S_p - I_p)\}, \qquad (13)$$

where *ref* is the albedo I_d, I_p, and S_p are the direct solar insolation, direct solar insolation on the horizontal plane, and global solar insolation on the horizontal plane, respectively. The diffuse solar insolation $(S_p - I_p)$ is considered as isotropic; Kondo's formulae (Kondo, 1994) were used for I_d and S_p. The terms with Σ are the reflection from other surfaces; s_{vfj}, r, and s_{wbj} are, respectively, the sky-view factor, the angle factor between the ray of direct insolation and each surface, and the view factor between the surface that reflects the shortwave radiation and the surface under consideration. $s_{vf} = r = 1$, and $s_{wb} = 0$ when there are no buildings; s_{vf}, r, and s_{wb} are not calculated precisely but, rather, are obtained with some geometric approximations (Kondo and Liu, 1998). Further formulations for them are given in the Appendix. R_{NS} is first defined for opaque buildings. The rates of reflection and transmission through the buildings are then considered according to $P_b(z)$. That is, part of the direct insolation $(1 - P_b(z))I_d$ can penetrate the

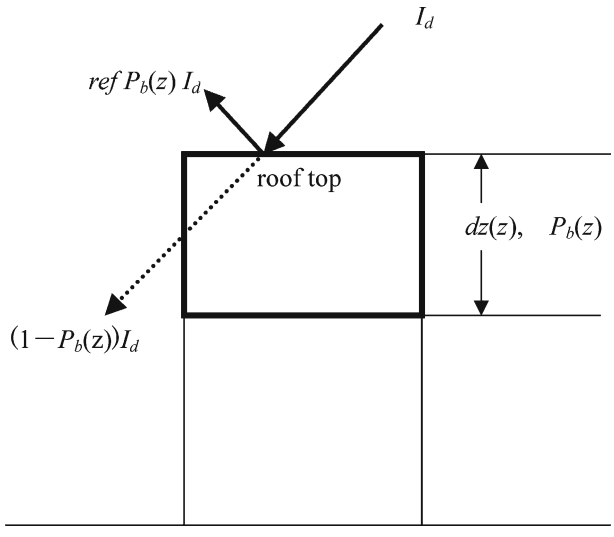

Figure 2. Direct insolation partly penetrates the building when $P_b(z) < 1$.

building, $(1 - ref)P_b(z)I_d$ is used to decide the heat budget at the building surface, and $refP_b(z)I_d$ is reflected (Figure 2). The same idea was also adopted for the calculation of diffuse (reflected) insolation.

The longwave flux from the atmosphere and re-emission from each surface are considered,

$$R_{NL} = \varepsilon_S s_{vf} L_a - \varepsilon_S \sigma T_w^4 + \sigma \sum_j (\varepsilon_{oj} T_{oj}^4 s_{wbj}), \tag{14}$$

where L_a is the longwave radiation from the atmosphere and is considered as isotropic. Kondo's formulae (Kondo, 1994) were also used for L_a. σ is the Stefan-Boltzmann constant, and ε_S is the emissivity of the surface under consideration. The terms with Σ are the longwave emission from other surfaces, where ε_{oj} and T_{oj} are the emissivity and surface temperature of other surfaces, respectively (Appendix A). Again, re-emission is considered only once. R_{NL} is also defined for opaque buildings first, and the rates of re-emission and transmission through the buildings are considered according to $P_b(z)$.

2.3. Surface fluxes

The sensible heat flux Q is calculated with Jurges's formulation (Jurges, 1924; McAdams, 1954) for a rough surface when the surface temperature is higher than the air temperature,

$$Q = \alpha(T_S - T_a), \tag{15}$$

where T_a is the temperature of the atmosphere and

$$\alpha = \begin{cases} 6.15 + 4.18U & U \leq 5\,\mathrm{m\ s^{-1}} \\ 7.51U^{0.78} & U > 5\,\mathrm{m\ s^{-1}} \end{cases}. \tag{16}$$

When $T_S < T_a$, the usual Monin-Obukhov (MO) theory is used for both horizontal and vertical surfaces because Equation (15) may overestimate the flux in stable conditions. The MO theory is also used to calculate the momentum flux (Kondo, 1975, 1994) with roughness lengths of 0.1 m and 0.0041 m specified for the momentum in all conditions and potential temperature for $T_S < T_a$, respectively, on each surface.

For the calculation of the latent heat flux, plant canopy conductance is introduced. Then,

$$\frac{E}{\rho} = \left(\frac{G_a G_S}{G_a + G_S}\right)(q_{vS}(T_S) - q_v(T_a)), \tag{17}$$

where G_a is the aerodynamic conductance, G_S, the plant canopy conductance, and $q_{vS}(T_S)$, the saturated specific humidity at T_S.

The heat storage in the wall of the buildings and in the ground is calculated using a one-dimensional thermal conduction equation,

$$\frac{\partial T_w}{\partial t} = \frac{\partial}{\partial n}\left(\kappa_w \frac{\partial T_w}{\partial n}\right). \tag{18}$$

Here, $\partial/\partial n$ means the derivative normal to the surface, and κ_w is the thermal diffusivity of the wall or the ground. Sixteen layers are used for walls, and 48 layers are used for the ground. Both fixed temperature and insulated boundary conditions can be used at the inside of the wall or at the bottom of the ground layer.

The surface of the roof, ground, and wall at each level can be further divided into three pieces, in which different albedo and plant canopy conductance can be specified. The total heat and moisture flux is aggregated with the weight of the area fraction of each piece.

3. Basic Results from the Off-line Canopy Model

In this section, results from the off-line canopy model are investigated. The model is one-dimensional, and the vertical grid intervals are basically 3 m from ground to 30 m, 5 m from 35 m to 150 m, and 10 m from 160 m to 300 m; the interval then increases up to 2350 m.

3.1. Averaged albedo over an urban area

The averaged albedo over an urban area is different from the albedo of the material surface itself. Here, the averaged albedo calculated in the canopy model is compared with the block canyon model experiment results of Aida (1982). Aida used 100 cubic concrete blocks of 0.15 m width that were distributed in a square pattern with separation 0.15 m, and measured the insolation reflected at 0.3 m above them. The surface albedo of the individual block surface was 0.38.

The averaged albedo over a block canyon is calculated with our off-line model under a similar condition to that in Aida's model experiment. The date and location were the same as those in the experiment, 15 June and Yokohama in Japan, respectively. In the present canopy model, the averaged albedo is calculated over cubic building blocks, whose width and separation are both 15 m. The averaged albedo is calculated from the integrated value of the total shortwave radiation received over the entire surface and the net shortwave radiation integrated over the entire surface in a unit canopy (Figure 2). Figure 3 shows the result from the calculation with Figure 4 in Aida (1982). The averaged albedo at noon in the calculation is 0.29, and this value coincides well with the albedo observed by Aida. However, the dependency

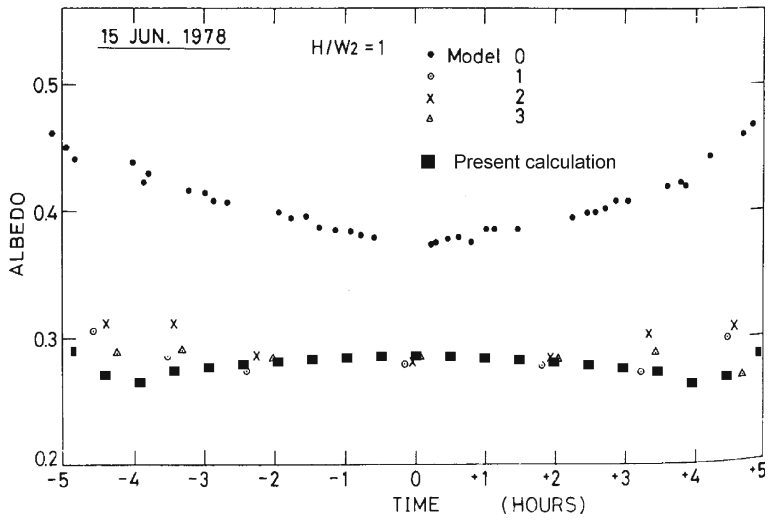

Figure 3. Time variation of canopy albedo with cubic buildings, calculated under the same condition as in Aida (1982)'s Figure 4, model 3.

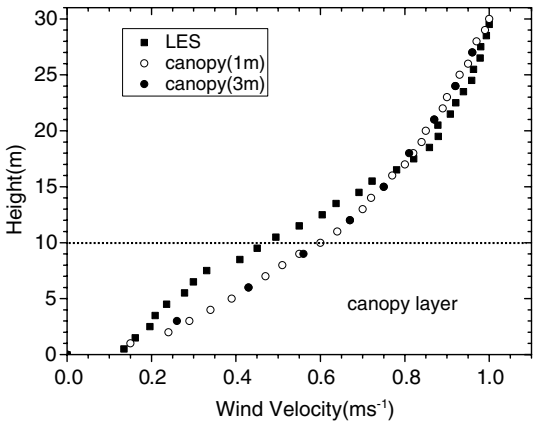

Figure 4. Comparison of the wind profile between large-eddy simulation (LES) and the canopy model. The wind velocity is normalized at 30 m. The results with grid intervals of both 1 m and 3 m from the canopy model are plotted in the figure.

of the albedo on the solar zenith angle is slightly different at hours ± 2 to 3. The numerical calculation of Aida and Gotoh (1982), which was a two-dimensional calculation with the Monte-Carlo method, showed that a minimum albedo was evident at an intermediate solar zenith angle, which was similar to the present calculation, but they attributed the minimum to the specular reflection from the surfaces in the canyon. The findings conflict because the specular reflection was not considered in the present study.

Figure 3 shows that the difference between the calculation and Aida's experiment is not very large in the present model.

3.2. Wind profile

The wind profile in and above the canopy is usually complex. Inoue and Kondo (1998) analyzed the three-dimensional flow in and above the building canopy using a large-eddy simulation (LES) model. They used the same LES model as Nakanishi (2000) except for the radiation process. Because only the averaged wind profile is obtained in the canopy model, the averaged wind profile in the LES model was compared with the results of the present canopy model. Inoue and Kondo calculated several cases, and, here, calculations around cubic buildings with a width of 10 m and separated by 20 m in a lattice with cyclic boundary conditions in neutral stability are compared. The top boundary is set at 30 m, and the wind velocity in the longitudinal direction is 1.0 m s^{-1}. The wind profile calculated from the canopy model is compared in Figure 4. The wind profile from the LES model is averaged over the transversal plane at the centre of the building in a longitudinal direction. Parameter c in Equations (1), (2), and (9), which depends on the volume density of the building in a canopy grid, is derived from a wind-tunnel experiment (Maruyama, 1991; Hagishima et al., 2001). Maruyama (1991) mounted many cubic roughness blocks in a staggered form in the wind tunnel to investigate the floor drag force. He then compared the force with that obtained from a numerical experiment with a two-dimensional k-ε equation

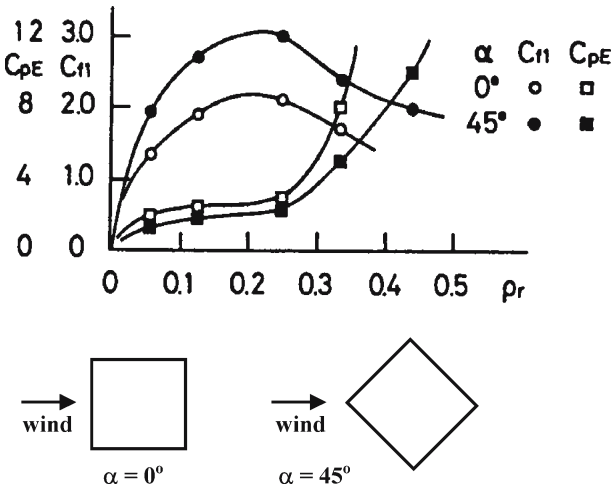

Figure 5. Variation of the parameters C_{f1} and C_{rE} with roughness density ρ_r (Maruyama, 1991); C_{pE} is a parameter used in the additional term for drag in the ε equation ($C_{\rho E} k^{\frac{3}{2}} L^{-1}$); k is the turbulent energy, and L is the scale length.

system (a similar equation system is shown in, e.g., Vu et al., 2002) with the drag force $\frac{1}{2}C_{f1}a_{x1}U|U|$ in the momentum equation, where $a_{x1} = b/\{(d+b)^2 - b^2\}$ in the present notation, and determined the coefficient C_{f1} as a function of the roughness density ($=b^2/(d+b)^2$ in the present notation; Figure 5). Hagishima et al. (2001) extended the comparison of the wind-tunnel experiment with a numerical experiment for a case in which the roughness blocks were mounted in a lattice. They concluded that the difference due to the arrangement of the roughness blocks is rather small. In our case, the buildings are spaced in a lattice, and we adopted $c = \frac{1}{2}, C_{f1} = 0.9$ from Figure 5.

The wind speed calculated in the canopy model is slightly underestimated above the canopy and overestimated in the canopy. The profile obtained from the canopy model does not depend on the grid interval except near the surface.

3.3. Daily course of the temperature in the canopy

The daily course of the temperature at 3 m height in the canopy is calculated in two cases without an anthropogenic heat source. In case 1, there is no building; case 2 involves cubic buildings with $b = h = 30$ m with a separation of 30 m, i.e., $d = 30$ m. The thickness of the building wall and roof was set at 0.2 m, and the temperature at the inside of the wall was fixed at 25 °C. Insulated material was used in the wall, and the lower boundary condition was set at 1.44 m under the ground. The parameters used in the calculation are shown in Table I. No vegetation was introduced on any of the surfaces. Solar insolation and longwave radiation from the atmosphere were assumed as of mid-July in Tokyo, Japan (139°46′ E, Lat. 35°40′ N). A geostrophic wind of 10 m s^{-1} and an initial lapse rate of 0.004 Km^{-1} were introduced.

TABLE I

Surface parameters used in case 1–4.

Surfaces	Albedo	Volumetric heat capacity (J m^{-3} K^{-1})	Thermal conductivity (J m^{-1} s^{-1} K^{-1})
Ground (0–0.36 m)	0.2	2.01×10^6	2.28
(0.36–1.44 m)	–	1.74×10^6	1.00
Wall (0.13–0.17 m)	–	0.20×10^6	0.23
(0–0.13 m, 0.17–0.2 m)	0.4	2.01×10^6	1.00
Roof (0.13–0.17 m)	–	0.20×10^6	0.23
(0–0.13 m, 0.17–0.2 m)	0.2	2.01×10^6	1.00

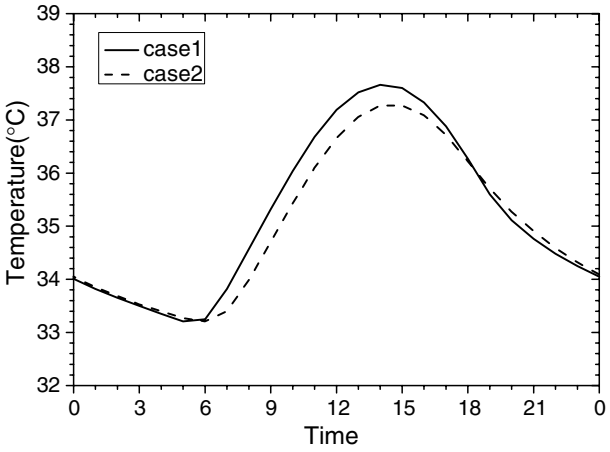

Figure 6. Daily variation of the air temperature at 3 m above the ground in the canopy. Case 1: no building. Case 2: cubic buildings with $b = h = 30$ m, $d = 30$ m.

The calculation was executed for 6 days, and the results of the last day, when the daily course was nearly in a periodic steady state, are shown in Figure 6. The figure shows the daily variation of the air temperature at 3 m above the ground in the canopy. Figure 6 demonstrates that the urban canopy lowers the maximum temperature, decreases the amplitude of the daily course, and delays the start of the increase in temperature. This is due to a smaller amount of total insolation reaching the building canyon in case 2 than in case 1. The cooling rate in the late afternoon was smaller in case 2 than in the case without buildings, and is due to the trapping of longwave radiation inside the canopy. Our canopy model reproduces these thermal characteristics well; however, the temperature inside the canopy depends strongly on the surface condition and materials.

3.4. Location of the anthropogenic heat source

Finally, the difference in the canopy temperature due to the difference in the level of the anthropogenic heat source is investigated. The condition of case 2 in the previous section is used, and an anthropogenic heat source is introduced. The level of the anthropogenic heat source is 3 m in case 3 and 30 m (on the roof) in case 4. Here, only sensible heat is considered. About 100 W m^{-2} for 0800–1800 LST and 20 W m^{-2} for other times are given (the same amount of anthropogenic heat is introduced in cases 3 and 4). Figure 7 shows the daily course of the temperature. The temperature at 3 m above the ground in the daytime increases by 1.5 K in cases with an anthropogenic heat source. However, if the heat source is located over the canopy, the temperature increase at the bottom of canopy is reduced by half.

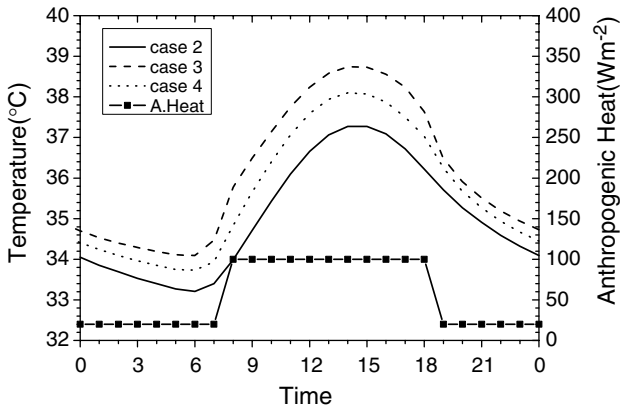

Figure 7. Daily course of the temperature with anthropogenic heat. The level of the anthropogenic heat source is 3 m in case 3 and 30 m (on the roof) in case 4. 100 W m^{-2} for 0800–1800 LST and 20 W m^{-2} for other times are given.

4. Linkage with a Mesoscale Model

The results of a one-dimensional model tend to overestimate the effects of urbanization because the model assumes that the same urban structure extends over an infinite area. Here, we combine the canopy model with a three-dimensional mesoscale model and compare it with the observations. The mesoscale model used is NIRE-MM (Kondo, 1989, 1995). In the present paper, we only examined the combination of a mesoscale model and a canopy model without anthropogenic heat discharge. Further investigations will investigate the combination of the present canopy model with a building energy-use model that calculates the anthropogenic heat discharge dynamically.

The same method as that of Martilli et al. (2002) is used for the data transfer from a mesoscale model to a canopy model. They interpolated fluxes onto the grid level of a mesoscale model from the grids of a canopy model. Here, we interpolate the temperature or wind itself from the canopy grid levels to the mesoscale grid levels.

5. Comparison with the Observation in Tokyo

The results of the on-line canopy model and the comparison with observations in the business district in Tokyo are shown in this section. The observation area is Kanda (Figure 8); a 200 m square area was selected, and the temperature at six points in the area (1.0 m height) was observed every 30 min (data for every hour are shown in Figure 9). The observations were carried

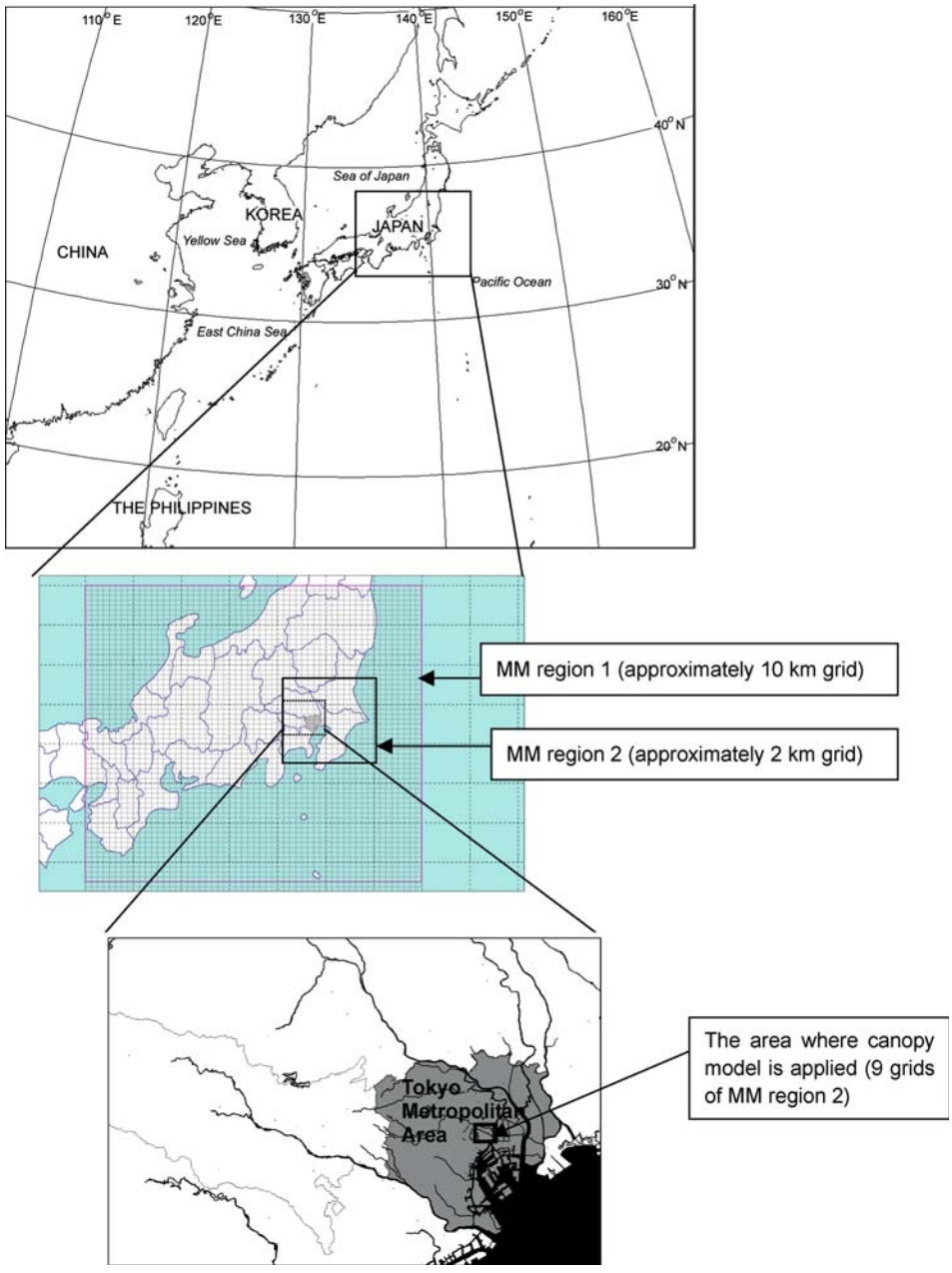

Figure 8. Domain of the calculation. The canopy model is applied to nine grids of the nested mesoscale model.

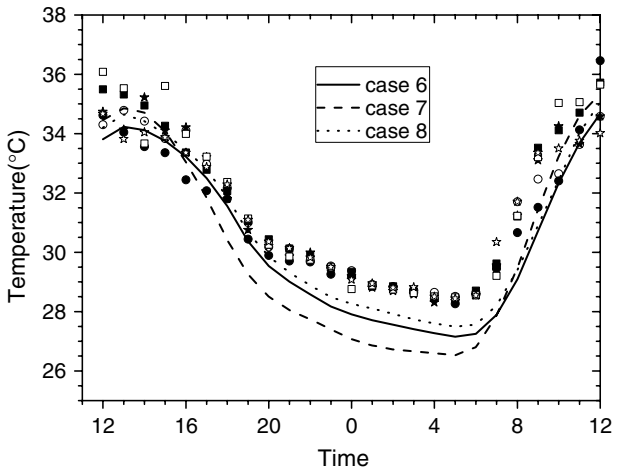

Figure 9. Comparison between the calculations of the temperature at 1.0 m (cases 6–8; lines) and observation at 1.0 m (symbols) on the roadside. Observations are plotted every hour.

out for 24 hours from noon on 10 August (Saturday) to noon on 11 August (Sunday) 2002. This period was the beginning of the Japanese summer holidays (the Bon Festival), during which most offices were closed. JMA GPV-MSM data (JMA, 2002) were used to drive the mesoscale model by the nudging method. The mesoscale model was one-way nested from a 10-km grid to a 2-km grid; then, the canopy model was linked with nine grids around the grid in which the observation was carried out (Figure 8). One canopy model is linked with one grid in the mesoscale model. The momentum, sensible heat, and latent heat fluxes in the mesoscale model were calculated with the same method as in Kondo et al. (2001) by using land-use data (Japan Map Center: http://www.jmc.or.jp) and a vegetation map of Japan (Biodiversity Center of Japan: http://www.biodic.go.jp). Anthropogenic heat was not introduced because of the holiday period. Calculations of the canopy model performed in

TABLE II
Parameters of the surfaces for the on-line calculation.

Surfaces	Albedo	volmetric heat capacity (J m^{-3} K^{-1})	thermal conductivity (J m^{-1} s^{-1} K^{-1})
Ground (0–0.36 m)	0.1	2.06×10^6	0.73
(0.36–1.44 m)	–	1.74×10^6	1.00
Wall and roof (0.16–0.2 m)	–	0.06×10^6	0.04
(0–0.16 m)	0.2	2.01×10^6	2.28
Window (30% of wall)	0.4	–	–

TABLE III
Canopy parameters used in case 6.

Level(m)	Pb
0–1	1
2–3	1
3–6	0.9429
6–9	0.8393
9–12	0.8393
12–15	0.767
15–18	0.6981
18–21	0.5976
21–24	0.5976
24–27	0.5203
27–30	0.4199
30–35	0.2871
35–40	0.1028
40–45	0.0261
45–50	0.0122
50–55	0.0096
55–60	0.0096
60–	0.0

$b = 12.7$ m, $d = 7.2$ m

this section employed the parameters shown in Table II for ground and building. The same data for the floor density distribution and other parameters for the canopy model are used for all nine grids, which are derived from a 500-m square area around the observation area, and the values are shown in Table III. No heat flux is assumed from the window surface.

Three cases are calculated. The canopy model with the floor density distribution given in Table 3 is used in case 6 (control run). No buildings are introduced in case 7. Case 8 is the same as case 6 except that the building height is fixed at 23.0 m, which is the average height of the buildings in the observation area. The volume roughness density of the buildings ($=\frac{b^2}{(d+b)^2}$) in this area is 0.41, and the corresponding $2c = C_{f1}$ is 1.4 for $\alpha = 0°$ and 2.1 for $\alpha = 45°$ from Figure 5. Since the relationship between the orientation of the building and the wind direction may be random in an urban area, we adopted $2c = 1.8$ (average). The calculation starts at 0900 JST, 7 August 2002. Figure 9 is a comparison between the calculations of the temperature at 1.0 m above the ground (cases 6–8) and the observation at 1.0 m on the roadside. The temperature calculated with a canopy model (cases 6, 8) is lower in the

morning and in the early afternoon and higher in the late afternoon and at night than that without a canopy model (case 7). The difference between cases 6 and 8 is small, but the temperature in case 8 is slightly higher than that in case 7 due to weaker ventilation effects in case 8. The observed temperatures are more scattered in the daytime than at night. The predicted temperature of cases 6 and 8 is lower at night than the observed temperature, but both calculations with a canopy model give a much better result than that without a canopy model at night. The low temperature at night, even with a canopy model, may result from the fact that nine canopy grids are insufficient to describe the total urban effects in Tokyo. Another possibility is that there

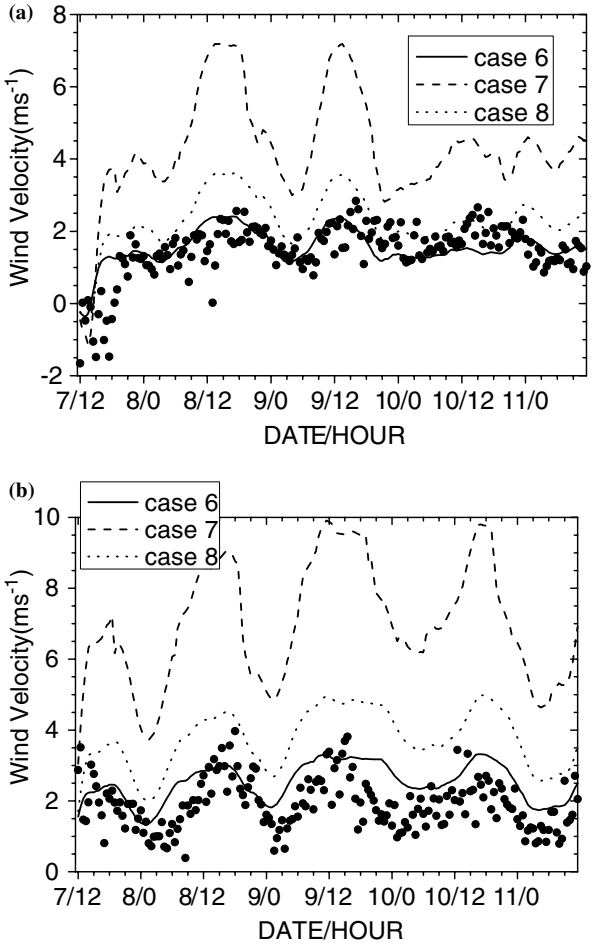

Figure 10. Wind velocities at 30 m in cases 6, 7, and 8 from Aug. 7, 1200, to August 11, 1200. The calculated velocities (lines) are compared with the observation (dots) at the roof of a nine-storey building. (a) *u* component and (b) *v* component.

should be anthropogenic heat even during the summer holiday period and that the lowest temperature is underestimated. These issues should be clarified in the near future.

Figure 10a, b shows the calculated wind velocity at 30 m, which is compared with the observation at the roof of a nine-storey building (point observation). In this period, the wind direction is almost south-west, and no higher building is upstream within 150 m of the observation point. The wind speed calculated in cases 7 and 8 is stronger than both that in case 6 and with the observed wind speed. When the floor density distribution is considered, significantly better results for the wind speed are obtained. However, the wind direction, even in case 6, is slightly different from that of the observation. This may be due to the unrealistic consideration of the street and building orientations.

6. Conclusions

A multilayer one-dimensional canopy model was developed to analyze the relationship between urban warming and the increase of energy consumption in a big city, and its basic performance was investigated. The albedo of the urban area and the wind profile in the simplified urban canopy calculated with an off-line canopy model were compared with the results from physical and more precise numerical calculations, and it was confirmed that the difference between the present canopy model and other more precise models is small. The basic thermal characteristics of the urban canopy were also investigated. The temperature near the surface decreases slowly from afternoon to evening with a canopy structure. The temperature increase in the morning is delayed, and the maximum temperature decreased slightly in the calculation that included the canopy model. When the anthropogenic heat sources were located near the ground in the canopy, the temperature near the surface increased.

The canopy model was connected with a mesoscale meteorological model, and on-line calculations were performed during the holiday period of 10 and 11 August 2002 for Tokyo, Japan, without anthropogenic heat. One of the characteristics of the present canopy model is to consider the floor density distribution of the buildings in both mechanical and radiation processes. The temperature calculated with a canopy is underestimated for the minimum temperature, in comparison with the observation; however, the temperature at night is improved with a canopy model. The temperature difference due to the canopy structure difference is small. The wind velocity calculated using the canopy model that included a floor density distribution gave the best agreement with the observed wind velocity at the top of a building.

Acknowledgements

This study was supported by the Proposal-Based New Industry Creative-Type Technology R & D Promotion Program from the New Energy and Industrial Technology Development Organization (NEDO) of Japan and by the Ministry of the Environment, Japan. Dr. Ryozo Ooka of the University of Tokyo is acknowledged for his contribution to the present research through his participation in the discussion of the radiative process.

Appendix A

A.1. Shortwave calculation in the canopy

We did not conduct an exact calculation of the radiation, as this is one of the most time-consuming parts of the model. Direct and diffuse insolation were separately considered and were calculated using Kondo's formulae (Kondo, 1994).

A.1.1. *Rooftop*

We consider the probability that the roof surface is protected from direct insolation by the shadow of the surrounding buildings. Figure A1 shows the

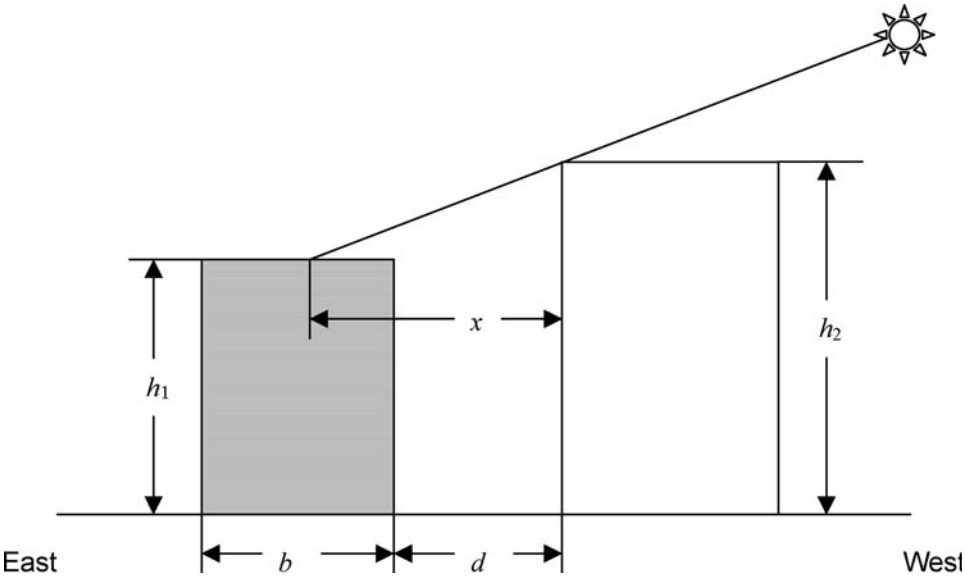

Figure A1. Path of the direct insolation to the roof of a building (east-west cross-section).

cross-section of the east–west direction through the centre of the buildings. x is the length of the shadow of the neighbouring building in the east–west direction at the rooftop level, h_1. If $x < d$, there is no shadow on the roof. The same idea is used in the north–south direction, and y is the length of the shadow of the neighbouring building in the north–south direction. Then, we assume the area of the shadow from neighbouring buildings as,

$$A_r = \min\{(x-d)(y-d), b^2\}\frac{b}{d+b} \quad \text{for } x > d \text{ and } y > d. \tag{A1}$$

The last term $\frac{b}{d+b}$ is added because many buildings stand at intervals of d in each direction.

When $h_2 > h_1$,

$$x = (h_2 - h_1)\tan\theta\sin\phi, \tag{A2}$$

$$y = (h_2 - h_1)\tan\theta\cos\phi, \tag{A3}$$

where θ is the solar zenith angle and ϕ is the hour angle ($=0$ at noon). We assume that part of the solar insolation passes through the building depending on the floor density distribution; in other words, the direct insolation reaching the rooftop is multiplied by the factor

$$\frac{A_r}{b^2}\{1 - P_b(z_n)\}, \tag{A4}$$

where z_n is the level at which direct insolation passes through the neighbouring building.

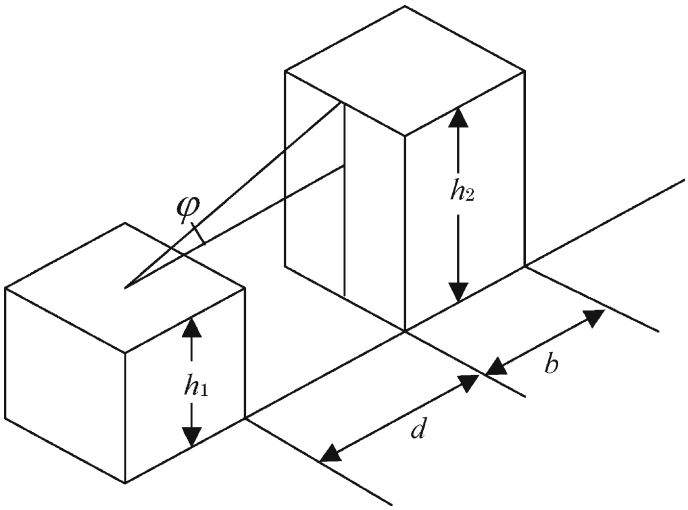

Figure A2. Elevation angle from the centre of the building under consideration to the centre of the top edge of a neighbouring building.

A sky-view factor at the centre of roof is used to obtain the diffuse solar insolation on the roof. φ is defined as the elevation angle from the centre of the building under consideration to the centre of the top edge of the neighbouring building shown in Figure A2. If the building under consideration is surrounded by a circular building with a height of h_2, then the sky-view factor is $\frac{1}{2}(1+\cos 2\varphi)$. In our consideration, the building is not circular but, rather, a rectangular building with a square bottom, and these buildings stand at intervals. We assume the sky-view factor as (Figure A3),

$$1-\frac{2}{\pi}(1-\cos 2\varphi)\arctan\left\{\frac{\frac{b}{2}}{\frac{b}{2}+d}\right\}. \tag{A5}$$

For the building under consideration, the shading effect only from the surrounding four buildings (located to the north, south, east and west) was taken into account.

Further shortwave radiation received at the roof is the reflection from the walls of buildings that are higher than those under consideration. We assume that the radiation is at the centre of the roof. The wall of a neighbouring building is divided vertically into n pieces, and the radiation from a wall piece between h_{j+1} and h_j is considered (Figure A4). The elevation angle for the

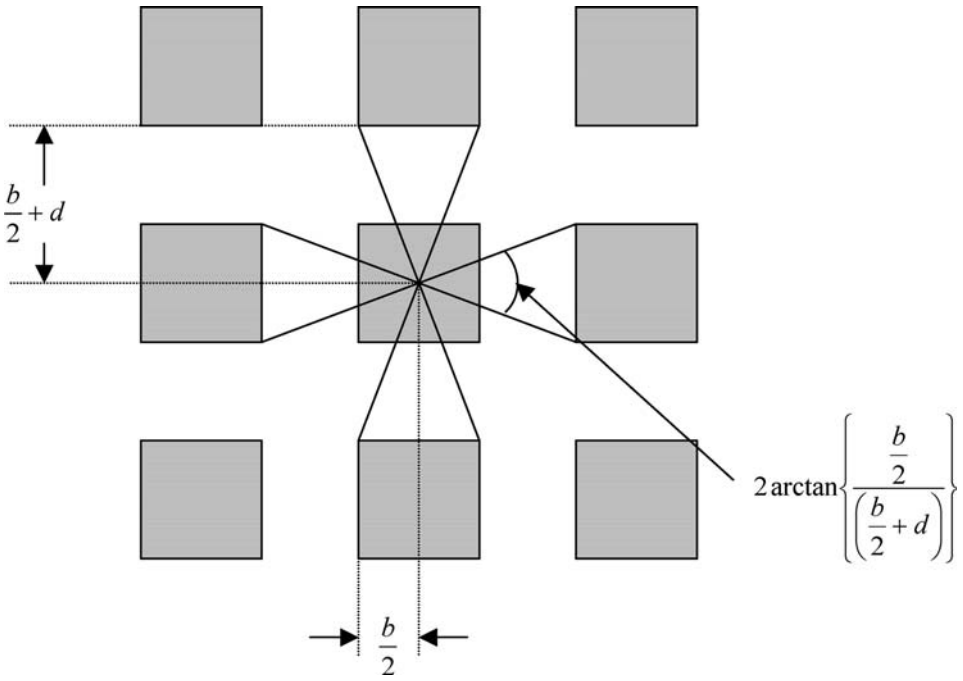

Figure A3. Angle of the width of neighbouring buildings.

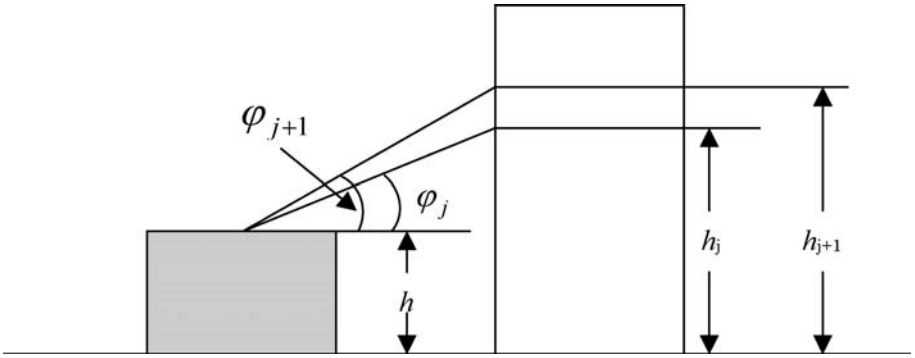

Figure A4. Elevation angle for the centre of the edge at level h_j of a neighbouring building.

centre of the edge at level h_j of a neighbouring building is

$$\varphi_j = \arctan\left\{\frac{h_j - h}{\frac{b}{2} + d}\right\}, \tag{A6}$$

and we assume that the reflected shortwave radiation received on the centre of the roof is

$$\cos\left(\frac{\varphi_j + \varphi_{j+1}}{2}\right)\left(\sin\varphi_j - \sin_{j+1}\right)\arctan\left\{\frac{\frac{b}{2}}{\left(\frac{b}{2} + d\right)}\right\}\frac{I_w}{\pi}, \tag{A7}$$

where I_w is the irradiance from the wall, which is assumed to be isotropic. Here, we disregard the dependency of reflection on the azimuth direction. I_w is also a function of the floor density, $P_b(h_j)$.

A.1.2. *Sidewalls*

The walls of the buildings face east, west, south, and north, and the direct insolation on each surface is,

$$\left.\begin{array}{ll} I_d \cos\varphi \sin\phi & \text{(east wall)} \\ -I_d \cos\varphi \sin\phi & \text{(west wall)} \\ I_d \cos\varphi \cos\phi & \text{(south wall)} \\ -I_d \cos\varphi \cos\phi & \text{(north wall),} \end{array}\right\} \tag{A8}$$

if there is no building other than that under consideration. Here, φ is the elevation angle, and ϕ is the hour angle of the sun. Only positive values are used.

We consider the two-dimensional street canyon first. If the neighbouring building is higher than the building being considered by Δh and the hour angle of the sun is ϕ, then

$$\Delta h = \frac{d}{\sin\phi}\tan\varphi_h \quad \text{for the walls facing east or west,}$$

$$\Delta h = \frac{d}{\cos\phi}\tan\varphi_h \quad \text{for the walls facing north or south,}$$

where φ_h is the elevation angle of the roof of the neighbouring building along the direction of the sun. If $\varphi > \varphi_h$, direct insolation reaches the wall under consideration. Actually, the buildings stand at intervals, so we assume the probability that the wall being considered is in the shade of the neighbouring building, $\frac{b}{d+b}$.

A sky-view factor to calculate the diffuse solar insolation from the sky is assumed to be $\frac{1}{2}\cos\left\{\arctan\left(\frac{d}{\Delta h}\right)\right\}$, as in the two-dimensional consideration. A two-dimensional consideration is also used for the reflection from the facing wall or road. The same idea as in the previous subsection about the floor density distribution is used for both direct and diffuse insolation.

A.1.3. *Ground*

We consider the proportion of the shadow on the ground to calculate the averaged direct insolation on the ground in a block. When the elevation angle of the sun is high, the shadow of the buildings does not reach the neighbouring building (Figure A5). Then, (x, $y < d$), the shadow area, is $(x+y)b$.

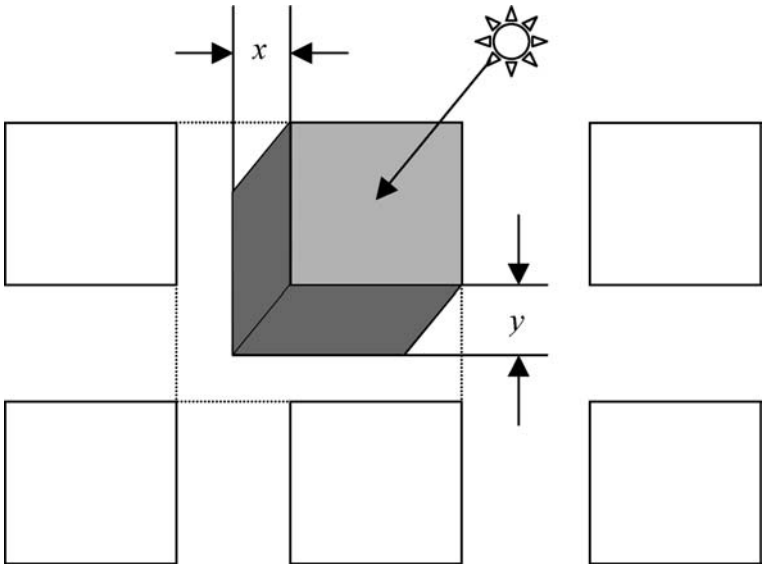

Figure A5. The shadow of the buildings does not reach the neighbouring building when the solar zenith angle is small.

When the elevation angle becomes low, the shadow of the building intrudes into the next block. We assume that the area of the shadow in the next block is,

$$\{\max(x-w,0)+\max(y-d,0)\}b \tag{A9}$$

on the ground. Because it is probable that the shadow touches the building wall or another shadow of a building in the nearby blocks, we assume such areas as

$$A_{gn}=\{\max(x-d,0)+\max(y-d,0)\}b\left\{\frac{b^2}{(d+b)^2}\right\}. \tag{A10}$$

Then, the total shadow area A_g may be $(x+y)b-A_{gn}$.

If $A_g > d^2+2bd$ (total area of the ground in a block), we assume $A_g = d^2+2bd$.

We divided the ground area into three parts: A, B, and C in Figure 1, and calculated the sky and other view factors at the centre of each area in order to calculate the diffused and reflected insolation. The approximated sky-view factor at the centre of area B is,

$$S_{vgB}=\frac{\int_{\frac{\pi}{4}}^{\frac{\pi}{2}}d\phi\int_{\varphi}^{\frac{\pi}{2}}\cos\varphi'\sin\varphi'd\varphi'}{\int_{\frac{\pi}{4}}^{\frac{\pi}{2}}d\phi\int_{0}^{\frac{\pi}{2}}\cos\varphi'\sin\varphi'd\varphi'}=\frac{\int_{\frac{\pi}{4}}^{\frac{\pi}{2}}d\phi\int_{\varphi}^{\frac{\pi}{2}}\cos\varphi'\sin\varphi'd\varphi'}{\frac{1}{2}\int_{\frac{\pi}{4}}^{\frac{\pi}{2}}d\phi\int_{0}^{\frac{\pi}{2}}\sin 2\varphi'd\varphi'}=\frac{\int_{\frac{\pi}{4}}^{\frac{\pi}{2}}d\phi\int_{\varphi}^{\frac{\pi}{2}}\cos\varphi'\sin\varphi'd\varphi'}{\frac{\pi}{8}}, \tag{A11}$$

which does not include the sky among the buildings in Figure A6. Similarly, the sky-view factor at the centre of areas A and C is,

$$S_{vgA}=\frac{\int_{0}^{\frac{\pi}{2}}d\phi\int_{\varphi}^{\frac{\pi}{2}}\cos\varphi'\sin\varphi'd\varphi'}{\int_{0}^{\frac{\pi}{2}}d\phi\int_{0}^{\frac{\pi}{2}}\cos\varphi'\sin\varphi'd\varphi'}=\frac{\int_{0}^{\frac{\pi}{2}}d\phi\int_{\varphi}^{\frac{\pi}{2}}\cos\varphi'\sin\varphi'd\varphi'}{\frac{1}{2}\int_{0}^{\frac{\pi}{2}}d\phi\int_{0}^{\frac{\pi}{2}}\sin 2\varphi'd\varphi'}=\frac{\int_{0}^{\frac{\pi}{2}}d\phi\int_{\varphi}^{\frac{\pi}{2}}\cos\varphi'\sin\varphi'd\varphi'}{\frac{\pi}{4}}, \tag{A12}$$

where $\varphi=\arctan\left(\frac{2h\cos\varphi}{d}\right)$.

These integrations are carried out numerically. We assume that the averaged sky-view factor on the ground S_{vg} is,

$$S_{vg}=\left(d^2S_{vgB}+2dbS_{vgA}\right)/\left(d^2+2db\right). \tag{A13}$$

For the reflection from the wall, we first calculate the radiation in the two-dimensional geometry. Then, the factor$(1-S_{vg})/(1-S_{vgA})$ is multiplied by the results.

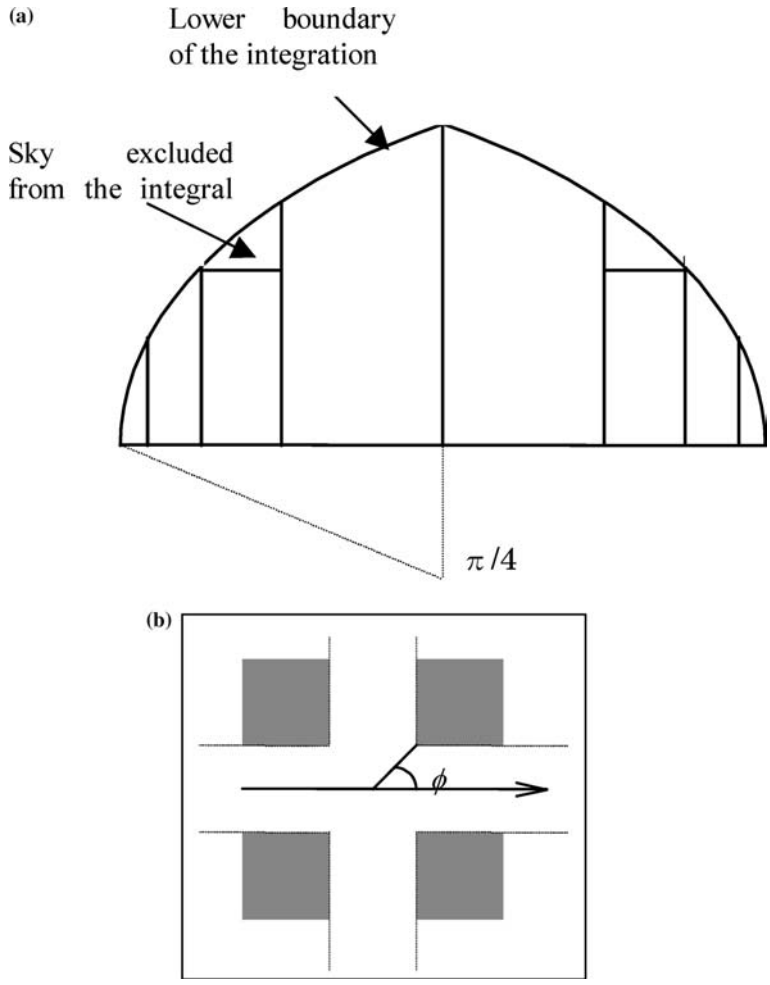

Figure A6. (a) A view of one block from the centre of the crossing road on the ground and lower boundary of elevation angle for the definite integral in Equation (A4). (b) Azimuth angle ϕ around the centre of crossing road for a building at a corner.

A.2. Longwave radiation

The longwave radiation of each part is the summation of that of the sky, building walls, and ground. We treat these as a function of view factors, which are the same as those calculated for shortwave (diffuse and reflected) radiation.

References

Aida, M.: 1982, 'Urban Albedo as a Function of the Urban Structure – A Model Experiment', *Boundary-Layer Meteorol.* **23**, 405–413.

Aida, M. and Gotoh, K.: 1982, 'Urban Albedo as a Function of the Urban Structure – A Two-dimensional Numerical Simulation', *Boundary-Layer Meteorol.* **23**, 415–424.

Akbari, H., Rosenfeld, A. H. and Taha, H.: 1990, 'Summer Heat Islands, Urban Trees, and White Surfaces', *ASHRAE Trans.* **96**, 1381–1388.

Ashie, Y., Vu, T. C. and Asaeda, T.: 1999, 'Building a Canopy Model for the Analysis of Urban Climate', *J. Wind Eng. Ind. Aerodyn.* **81**, 237–248.

Blackadar, A. K.: 1968, 'The Vertical Distribution of Wind and Turbulent Exchange in Neutral Atmosphere', *J. Geophys. Res.* **67**, 3085–3102.

Gambo, K.: 1978, 'Notes on the Turbulence Closure Model for Atmospheric Boundary Layers', *J. Meteorol. Soc. Jpn.* **56**, 466–480.

Hagishima, A., Tanimoto, J. and Katayama, T.: 2001, 'Experiment Study on the Validity of an Urban Canopy Model in and Above the Canopy Layer', *J. Archit. Plan. Environ. Eng.* **548**, 31–37(in Japanese).

Ichinose, T., Shimodozono, K. and Hanaki, K.: 1999, 'Impact of Anthropogenic Heat on Urban Climate in Tokyo', *Atmos. Environ.* **33**, 3897–3909.

Inoue, M. and Kondo, H.: 1998, 'A Study on the Effect of Anthropogenic Heat on the Temperature Distribution in the Urban Canopies', *J. Jpn. Soc. Atmos. Environ.* **33**, 93–108(in Japanese).

JMA: 2002, Outline of the Operational Numerical Weather Prediction at the Japan Meteorological Agency, Appendix to WMO Numerical Weather Prediction Progress Report, available from http://www.jma.go.jp/JMA_HP/jma/jma-eng/jma-center/nwp/outline-nwp/index.htm.

Jurges, W.: 1924, 'Der Warmeuberergang an einer ebenen Wand', *Gesundheight-Ingnierur* **19**, 1 (in German).

Kikegawa, H., Genchi, Y., Yoshikado, H. and Kondo, H.: 2003, 'Development of a Numerical Simulation System Toward Comprehensive Assessments of Urban Warming Countermeasures, Including Their Impacts upon the Urban Building's Energy-demands', *Appl. Energy* **76**, 449–466.

Kondo, J.: 1975, 'Air–sea Bulk Transfer Coefficients in Diabatic Conditions', *Boundary-Layer Meteorol.* **9**, 91–124.

Kondo, J. (ed.): 1994, *The Meteorology in Water Environment*, Asakura-shoten, Tokyo, 350 pp. (in Japanese).

Kondo, J. and Akashi, S.: 1976, 'Numerical Studies on the Two-dimensional Flow in a Horizontally Homogeneous Canopy Layer', *Boundary-Layer Meteorol.* **10**, 255–272.

Kondo, H.: 1989, *Description of NRIPR Mesoscale Model*, Technical Report No. 44, National Research Institute for Pollution and Resources, Tsukuba, Japan, 76 pp.

Kondo, H.: 1995, 'The Thermally Induced Local Wind and Surface Inversion over the Kanto plain On Calm Winter Nights', *J. Appl. Meteorol.* **34**, 1439–1448.

Kondo, H. and Liu, F. H.: 1998, 'A Study on the Urban Thermal Environment Obtained Through a One-dimensional Urban Canopy Model', *J. Jpn. Soc. Atmos. Environ.* **33**, 179–192(in Japanese).

Kondo, H., Saigusa, N., Murayama, S., Yamamoto, S. and Kannari, A.: 2001, 'A Numerical Simulation of the Daily Variation of CO_2 in the Central Part of Japan, Summer Case', *J. Meteorol. Soc. Jpn.* **79**, 11–21.

Kondo, H. and Kikegawa, H.: 2003, 'Temperature Variation in the Urban Canopy with Anthropogenic Energy Use', *Pure Appl. Geophys.* **160**, 317–324.

Kusaka, H., Kondo, H., Kikegawa, H. and Kimura, F.: 2001, 'A Simple Single-layer Urban Canopy Model for Atmospheric Models: Comparison with Multi-layer and Slab models', *Boundary-Layer Meteorol.* **101**, 329–358.

McAdams, W. H.: 1954, *Heat Transmission*, (3rd ed.). McGraw-Hill, New York, 532 pp.

Martilli, A.: 2002, 'Numerical Study of Urban Impact on Boundary Layer Structure: Sensitivity to Wind Speed, Urban Morphology, and Rural Soil Moisture', *J. Appl. Meteorol.* **41**, 1247–1266.

Martilli, A., Clippier, A. and Rotach, M. W.: 2002, 'An Urban Surface Exchange Parameterization for Mesoscale Models', *Boundary-Layer Meteorol.* **104**, 261–304.

Maruyama, T.: 1991, 'Numerical Simulation of Turbulent Boundary Layer over Complicated Surfaces Such as Urban Areas', *J. Wind Eng.* **47**, 81–81(in Japanese).

Masson, V.: 2000, 'A Physically-based Scheme for the Urban Energy Budget in Atmospheric Models', *Boundary-Layer Meteorol.* **94**, 354–397.

Murakami, S., Mochida, A., Kim, S., Ooka, R., Yoshida, S., Kondo, H., Genchi, Y., and Shimada, A.: 2000, 'Software Platform for the Total Analysis Wind Climate and Urban Heat Island. Integration of C.W.E. Simulation from Human Scale to Urban Scale, *Proc 3rd International Symposium on Computational Wind Engineering*, pp. 23–36.

Nakanishi, M.: 2000, 'Large-Eddy Simulation of Radiation Fog', *Boundary-Layer Meteorol.* **94**, 461–493.

Oke, T. R.: 1978, *Boundary Layer Climate*, Mathuen & Co. Ltd., New York, 372 pp.

Sorbjan, Z. and Uliasz, M.: 1982, 'Some Numerical Urban Boundary-layer Studies', *Boundary-Layer Meteorol.* **22**, 481–502.

Uno, I., Ueda, H. and Wakamatsu, S.: 1989, 'Numerical Modeling of the Nocturnal Urban Boundary Layer', *Boundary-Layer Meteorol.* **49**, 77–98.

Urano, A., Ichinose, T. and Hanaki, K.: 1999, 'Thermal Environment Simulation for Three-dimensional Replacement of Urban Activity', *J Wind Eng. Ind. Aerodyn.* **81**, 197–210.

Vu, T. C., Ashie, Y. and Asaeda, T.: 2002, 'A k–ε Turbulence Closure Model for the Atmospheric Boundary Layer including Urban Canopy', *Boundary-Layer Meteorol.* **102**, 459–490.

Watanabe, T. and Kondo, J.: 1990, 'The Influence of the Canopy Structure and Density upon the Mixing Length within and above Vegetation', *J Meteorol. Soc. Jpn.* **68**, 227–235.